



ACADÉMIE  
DES SCIENCES  
INSTITUT DE FRANCE

# *Comptes Rendus*

---

## *Physique*

Ian G. Moss


**Analogue black holes and scalar-dilaton theory**

Published online: 3 December 2024

**Part of Special Issue:** Simulating gravitational problems with condensed matter analog models : a special issue in memory of Renaud Parentani (1962-2020)

**Guest editors:** Jacqueline Bloch (Université Paris-Saclay, CNRS, Centre de Nanosciences et de Nanotechnologies, Palaiseau, France), Iacopo Carusotto (Pitaevskii BEC Center, INO-CNR, Trento, Italy) and Chris Westbrook (Laboratoire Charles Fabry de l'Institut d'Optique, Palaiseau, France)

<https://doi.org/10.5802/crphys.211>

 This article is licensed under the  
CREATIVE COMMONS ATTRIBUTION 4.0 INTERNATIONAL LICENSE.  
<http://creativecommons.org/licenses/by/4.0/>



*The Comptes Rendus. Physique are a member of the  
Mersenne Center for open scientific publishing*  
[www.centre-mersenne.org](http://www.centre-mersenne.org) — e-ISSN : 1878-1535



Research article / *Article de recherche*

Simulating gravitational problems with condensed matter analog models : a special issue in memory of Renaud Parentani (1962-2020) / *Simuler des problèmes gravitationnels avec des modèles analogues en matière condensée : un numéro spécial en mémoire de Renaud Parentani (1962-2020)*

# Analogous black holes and scalar-dilaton theory

## *Analogues de trous noirs et théorie scalaire-dilaton*

Ian G. Moss <sup>a</sup>

<sup>a</sup> School of Mathematics, Statistics and Physics, Newcastle University, Newcastle Upon Tyne, NE1 7RU, UK  
*E-mail:* [ian.moss@newcastle.ac.uk](mailto:ian.moss@newcastle.ac.uk)

**Abstract.** This note analyses the long wavelength dynamics of a two horizon analogue black hole system in one spatial dimension. By introducing an effective scalar-dilaton model we show that closed form expressions can be obtained for the time-dependent Hawking flux and the energy density of the Hawking radiation. We show that, in the absence superluminal modes, there is a vacuum instability. This instability is recognisable to relativists as the analogue to the destabilisation of the Cauchy horizon of a black hole due to vacuum polarization.

**Résumé.** Cette note analyse la dynamique des grandes longueurs d'onde d'un système analogue de trous noirs à deux horizons dans une dimension spatiale. En introduisant un modèle scalaire effectif du type dilaton, nous montrons que des expressions analytiques peuvent être obtenues pour le flux de Hawking dépendant du temps et la densité d'énergie du rayonnement de Hawking. Nous montrons qu'en l'absence de modes superluminaux, il existe une instabilité du vide. Cette instabilité est reconnaissable pour les relativistes comme l'analogie de la déstabilisation de l'horizon de Cauchy d'un trou noir due à la polarisation du vide.

**Keywords.** Black holes, Bose–Einstein condensates, analogue gravity.

**Mots-clés.** Trous noirs, condensats Bose–Einstein, gravité analogue.

**Funding.** The author has received financial support from the Science and Technology Facilities Council grant ST/T00584X/1.

*Manuscript received 5 April 2024, revised 4 July 2024, accepted 23 September 2024.*

## 1. Introduction

Laboratory analogues of Hawking radiation could provide insight into many of the outstanding questions surrounding black hole evaporation [1–3]. Bose–Einstein condensates (BEC) provide fertile ground for possible analogue models. The long wavelength perturbations of a condensate are described by an effective scalar field theory with a background metric. Given the appropriate background velocity field, the analogue metric can have horizons that produce Hawking radiation in the form of pseudo-quanta in the condensate field. This note focusses on one particular aspect of Hawking radiation, which is the stability of the Hawking stress-energy at the Cauchy, or innermost horizon, of a black hole.

Analogue models with two horizons are of particular interest because they were used in the first experiments that produced Hawking radiation in the laboratory [4, 5]. Early theoretical investigations of the two-horizon system by Corley and Jacobson [6] revealed the possible existence of a laser effect. If the effective scalar field theory has a dispersion relation of the form  $\omega^2 = k^2 + k^4/\Lambda^2$ , the Hawking radiation outside the horizons grows exponentially, implying an instability of the vacuum state. Later work, by Parentani and others, which did not rely on the WKB approximation used by Corley and Jacobson, found a more nuanced situation with evidence for a laser effect depending on the particular set-up [7, 8]. Following Steinhauer’s experiment, there have been a number of attempts to examine the laser phenomenon and reproduce the experimental results by solving the Gross–Pitaevski equation for the mean condensate field with various forms of noise added to mimic the quantum fluctuations [9–11]. The results appear to be rather dependent on the approach that is followed.

In this note, we focus only on the long wavelength dynamics of the two horizon system in one spatial dimension. The methods used are generalisations of the conformal methods introduced by Christensen and Fulling [12]. By introducing an effective scalar-dilaton model we shall see that closed form expressions can be obtained for the Hawking flux and energy density of the Hawking radiation. We shall show that, even when we drop the superluminal modes, there is a vacuum instability. This instability is recognisable to relativists as the analogue to the destabilisation of the Cauchy horizon of a black hole due to vacuum polarization [13, 14].

The Cauchy horizon has been of long-standing interest in relativity. Traversing the Cauchy horizon would allow views of the singularity inside the black hole and signal a breakdown of the cosmic censorship principle. Instability of the Cauchy horizon would in this respect be a desirable thing [15, 16], but there has been a recent reawakening of interest in the issue and the possibility that physical objects could traverse the Cauchy horizon unscathed [17, 18].

The results below describe in detail how energy accumulates on the analogue Cauchy horizon, usually referred to in analogue gravity context as the white hole horizon. The analysis is limited to long wavelength modes, but allows for density and sound speed variations. In practice, either the short wavelength modes or non-linearities will regularise the energy density at the analogue Cauchy horizon, but extending beyond long wavelengths requires a full mode analysis beyond the scope of the simple treatment presented here. Hopefully, the analysis below may help guide future numerical work that covers the dynamics on all scales.

## 2. The spacetime geometry

Analogue gravity is based on the fact that the velocity potential for waves in an Eulerian fluid satisfy the relativistic wave equation with an analogue metric, the Unruh metric [1]. In one dimension (1D),

$$ds^2 = \frac{a}{c} \left\{ - \left( c^2 - v_f^2 \right) dt^2 - 2v_f dt dr + dr^2 \right\}, \quad (1)$$

where  $v_f(r)$  is the background fluid velocity and  $c(r)$  is the sound speed. (It is convenient to take  $v_f < 0$  and  $c > 0$ .) The extra factor  $a(r)$  is the density in the Unruh metric, but in 1D the wave equation is independent of  $a$  and we can choose  $a$  as we wish.

The metric diagonalises using the time coordinate  $\tau = t + r_*$ , where

$$dr_* = \frac{v_f dr}{c^2 - v_f^2}. \quad (2)$$

Then the metric takes a Boyer–Lindquist form,

$$ds^2 = a \{-B(r)d\tau^2 + B(r)^{-1}dr^2\} \quad (3)$$

where

$$B(r) = \frac{c^2 - v_f^2}{c}. \quad (4)$$

Black hole horizons occur at the roots  $r_i$  of  $B(r) = 0$ , i.e.  $v_f = \pm c$ .



**Figure 1.** Schematic diagram of a two-horizon fluid flow with horizons at  $r_c$  and  $r_h$ .

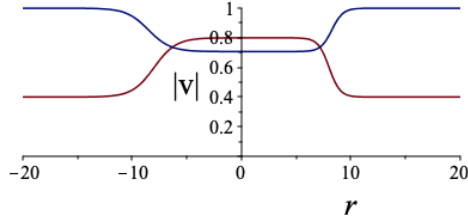


**Figure 2.** Plot of a typical two-horizon fluid flow with velocity  $v_f$  (blue) and sound speed  $c$  (red) with two horizons where  $v_f = -c$ .

The Penrose diagram for this spacetime is constructed from null Kruskal coordinates as follows. First, define a new stretched coordinate  $r^*$ ,

$$dr^* = \frac{c dr}{c^2 - v_f^2} \quad (5)$$

There are singularities in  $r^*$  at the horizons, but this definition can be used for the entire range of  $r$  providing we use a principle value prescription. Let  $\kappa_i = B'(r_i)/2 = c' + v_f'$ , then  $r^* \rightarrow -\infty$  at any horizon where  $\kappa_i > 0$  and  $r^* \rightarrow \infty$  at any horizon where  $\kappa_i < 0$ . In the region near the horizon, we define

$$U_i = -e^{-\kappa_i(\tau - r^*)}$$

$$V_i = e^{\kappa_i(\tau + r^*)}$$

These null coordinates vanish at the horizon  $r_i$  and the metric is regular there. They allow us to extend the metric across the horizon. In the Penrose diagram, lines of constant  $U_i$  and  $V_i$  have slope  $\pm 45^\circ$  respectively. The full Penrose diagram is constructed by patching these regions together to cover the entire range of  $r$ .

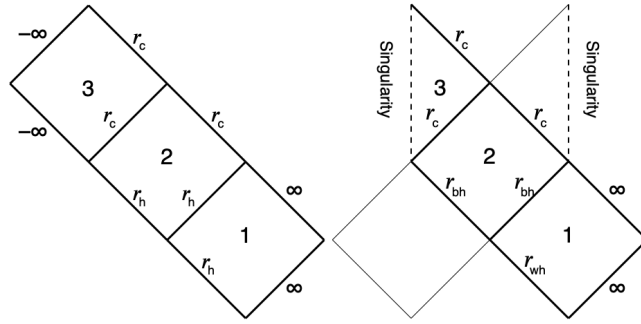


**Figure 3.** Penrose diagrams for the analogue black hole (left) and the rotating black hole (right). The horizons are labelled  $r_h$  and  $r_c$ . In region 2 of the analogue hole,  $r_c < r < r_h$ , right moving waves are left-moving in the original coordinates and so they end up dragged to the horizon  $r_c$ .

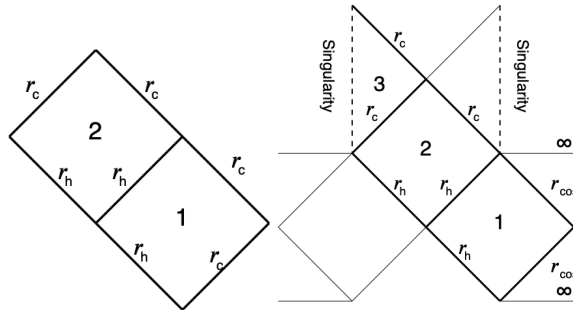


**Figure 4.** Penrose diagrams for the analogue black hole with a circular topology (left) and the rotating black hole in de Sitter space (right). The latter has an additional horizon, the cosmological horizon, at  $r = r_{cos}$ . In region 1 of the analogue hole, right moving waves travel round the circle and meet the horizon at  $r_c$ . The topology of regions 1 and 2 are the same in both cases if we unwind the circle and work with the periodic potential.

Figures 3 and 4 show the Penrose diagram for a flow which is superluminal between two fixed horizons  $r = r_c$  and  $r = r_h$ , of opposite surface gravity. There are two cases, a linear one with  $-\infty < r < \infty$ , and a circular topology with periodic potential. An odd feature is that each horizon appears multiple times in the Penrose diagram, depending in whether waves are approaching from the left or the right. The horizon at  $r_c$  is a Cauchy horizon for region 2, i.e. wave motion in region 3 cannot be predicted from initial data in region 2. Furthermore, waves falling in from region 1 “pile up” along the horizon at  $r_c$  [19]. Note that this horizon has some similarities also to a white hole, because null geodesics exit region 2 into region 3 across  $r = r_c$ . In the literature, the upflow horizon  $r_h$  is usually referred to as the black hole horizon and the downflow  $r_c$  as the white hole horizon.

Figure 3 shows the Penrose diagram of a four dimensional rotating black hole for comparison. The topology of the space spanned by the (compactified) Kruskal coordinates for regions 1 and 2 is very similar. The differences lie mostly in the future extensions of the spacetime beyond the Cauchy horizons. It seems reasonable to regard the horizon at  $r_c$  as an analogue to the Cauchy horizon of a black hole.

### 3. From BEC to scalar-dilaton theory

This part of the story is not new and is only told in outline [20, 21]. First, there is the action for the mean BEC field  $\psi(r, t)$ ,

$$S = \int \left\{ \frac{i}{2} \hbar \bar{\psi} \partial_t \psi - \frac{i}{2} \hbar \psi \partial_t \bar{\psi} - \frac{\hbar^2}{2m} \partial_r \bar{\psi} \partial_r \psi - \frac{1}{2} g (\bar{\psi} \psi)^2 + \mu \bar{\psi} \psi - V \bar{\psi} \psi \right\} dr dt, \quad (6)$$

where  $g$  is the effective self-coupling in one dimension and  $\mu$  sets the density scale. The inhomogeneous trapping potential  $V$  drives a background flow in the condensate. Potentials in the transverse directions (not shown here) confine the condensate so that it behaves as a 1D system. The action is expanded about the time independent background, which has velocity  $v$  and sound speed  $c$ ,

$$\psi = \sqrt{\rho} e^{i\theta} (1 + \delta\psi), \quad v = \hbar \partial_r \theta / m, \quad g\rho = mc^2 \quad (7)$$

At quadratic order, let  $\Psi = (\delta\psi, \delta\bar{\psi})^T$ , the perturbed action reads

$$S[\Psi] = \int \rho \left\{ \frac{i}{2} \hbar \Psi^\dagger \sigma_z (\partial_t + v \partial_r) \Psi + \frac{\hbar^2}{4m} \Psi^\dagger \partial_r^2 \Psi - \frac{1}{2} \Psi^\dagger \mathbf{H} \Psi \right\} dr dt \quad (8)$$

where  $\sigma_i$  are the Pauli matrices and

$$\mathbf{H} = g\rho \sigma_x + g\rho 1. \quad (9)$$

The field equation for the backgrounds  $\rho$  and  $v$  have been used. Next, diagonalise the matrix  $\mathbf{H}$ , by introducing the normalised eigenvectors  $u$  and  $u'$ , such that  $\sigma_z u = u'$ . Introduce (Bogoliubov) normal modes  $\varphi$  and conjugate momenta  $p$ ,

$$\Psi = -i\varphi u + \hbar^{-1} p u' \quad (10)$$

In these fields,

$$S[\varphi, p] = \int \rho \left\{ p (\partial_t + v \partial_r) \varphi - \frac{1}{2} \frac{\hbar^2}{2m} (\partial_r \varphi)^2 - \frac{1}{2\hbar^2} \left( \frac{\hbar^2}{2m} (\partial_r p)^2 + 2mc^2 p^2 \right) \right\} dr dt \quad (11)$$

Finally, consider the long wavelength limit where the field  $p$  is composed mainly of Fourier modes with  $k \ll \xi^{-1}$ , where the healing length  $\xi = \hbar/mc$ . For consistency, we should check if this is consistent with the Hawking radiation. The Hawking spectrum is in the desired wavelength range if  $k_B T_H \ll \hbar c / \xi$ . The formula for the Hawking temperature (see later) is  $k_B T_H \sim \hbar v_f$ , which implies that the background velocity field should not vary very much on the scale of the healing length. This not unreasonable in actual experiments.

In the long wavelength limit,  $p \approx \hbar^2 (2mc^2)^{-1} (\partial_t + v \partial_r) \varphi$ , and eliminating  $p$  gives

$$S[\varphi] = \frac{\hbar^2}{2m} \int \rho \left\{ \frac{1}{2c^2} [(\partial_t + v \partial_r) \varphi]^2 - \frac{1}{2} (\partial_r \varphi)^2 \right\} dr dt. \quad (12)$$

We rewrite the action in geometrical form by introducing the fluid metric,

$$g^{-1} |g|^{1/2} = c \left\{ -\frac{1}{c^2} (\mathbf{e}_t + v \mathbf{e}_r) \otimes (\mathbf{e}_t + v \mathbf{e}_r) + \mathbf{e}_r \otimes \mathbf{e}_r \right\}. \quad (13)$$

The action has a pseudo-geometrical form,

$$S[\varphi] = \frac{\hbar^2}{2m} \int \left\{ -\frac{1}{2} g^{\mu\nu} (\partial_\mu \varphi) (\partial_\nu \varphi) |g|^{1/2} \right\} \frac{\rho}{c} dr dt \quad (14)$$

In three spatial dimensions, the factors after the bracket can be absorbed by the inverse metric. However, in 1D this is not possible and the  $\rho/c = (\rho m/g)^{1/2}$  term is always present. The system can be viewed instead as a model with an external dilaton field  $\Phi$ ,

$$\Phi = -\frac{1}{4} \ln \left( \frac{\hbar^2 \rho}{4mg} \right). \quad (15)$$

Then

$$S[\varphi] = -\hbar \int \left\{ \frac{1}{2} g^{\mu\nu} (\partial_\mu \varphi) (\partial_\nu \varphi) e^{-2\Phi} \right\} |g|^{1/2} dr dt. \quad (16)$$

This is still a conformally invariant model, i.e. the field equations are invariant under rescaling of the metric and we can make an arbitrary choice of the factor  $a$  in the metric. Different choices would, however, have an effect on the energy density (see later).

In the  $(\tau, r^*)$  coordinate system, the field equation for  $\phi = e^{-\Phi} \varphi$  becomes

$$\partial_\tau^2 \phi - \partial_{r^*}^2 \phi + (\rho^{-1/4} \partial_{r^*}^2 \rho^{1/4}) \phi = 0 \quad (17)$$

Note that this equation is scattering problem with potential  $\rho^{-1/4} \partial_{r^*}^2 \rho^{1/4}$ . The Hawking flux from a single horizon in this model has a grey-body spectrum with transmission coefficients determined by the scattering potential. However, the potential is very small in flows where  $\rho$  only varies when close to the horizon.

#### 4. Scalar-dilaton theory

Much is known about scalar-dilaton theory in 2D because it was used to describe the back-reaction of Hawking radiation on the black hole spacetime [22–25] (the CGHS model). An effective action approach similar to the one used below has been used for analogue black holes [26, 27], but previous work has only been applied to a single horizon and without the dilaton field.

First off, note that the stress-energy tensor of the scalar  $\varphi$  is not conserved because of the external dilaton field  $\Phi$ . Fortunately, the action is in geometric form and we can apply general covariance to obtain the modified conservation rules. Consider an infinitesimal diffeomorphism  $\delta g_{\mu\nu} = 2\xi_{(\mu;\nu)}$  and  $\delta\Phi = \Phi^{;\mu} \xi_\mu$ , then covariance implies

$$\delta S = \int \left\{ 2 \frac{\delta S}{\delta g_{\mu\nu}} \xi_{(\mu;\nu)} + \frac{\delta S}{\delta \Phi} \Phi^{;\mu} \xi_\mu \right\} d\mu = 0 \quad (18)$$

Hence

$$\nabla_\mu T^\mu{}_\nu = \frac{\delta S}{\delta \Phi} \nabla_\nu \Phi \quad (19)$$

In the quantum theory, this becomes an operator equation and we have

$$\nabla_\mu \langle T^\mu{}_\nu \rangle = \frac{\delta \Gamma}{\delta \Phi} \nabla_\nu \Phi \quad (20)$$

where  $\Gamma[g_{\mu\nu}, \Phi]$  is the effective action with the external metric  $g_{\mu\nu}$  and dilaton field  $\Phi$ .

The most important result for completing the theoretical description is the trace anomaly. This was mired in controversy for a while, but in the end the correct result was given by Dowker [28]

$$\langle T^\mu{}_\mu \rangle = \frac{\hbar}{24\pi} (R - 6\Phi_{;\mu} \Phi^{;\mu} + 4\Phi_{;\mu}{}^{;\mu}) \quad (21)$$

Bousso and Hawking demonstrated that it is possible to write down an effective action which is consistent with the trace anomaly [29]. After correcting the trace anomaly in Bousso's work,

$$\Gamma = -\frac{\hbar}{48\pi} \int \left\{ \frac{1}{2} R \square^{-1} R - 6\Phi_{;\mu} \Phi^{;\mu} \square^{-1} R + 4\Phi R \right\} d\mu \quad (22)$$

The inverse d'Alembertian  $\square^{-1}$  is less problematic than may first appear. For example, in the fluid metric  $R = -\square \ln |aB|$ , and we apply the simple rule  $\square^{-1} \square = 1$ . This effective action has been used extensively in discussions of the back reaction of Hawking radiation, but it should be noted that this action is not an exact result. Nevertheless, we continue with this action as in previous work. The functional derivative

$$\frac{\delta \Gamma}{\delta \Phi} = -\frac{1}{12\pi} R - \frac{1}{4\pi} (\Phi^{;\mu} \square^{-1} R)_{;\mu} \quad (23)$$

We can now combine with (20) to obtain a complete set of equations that can be solved for the stress tensor  $\langle T^\mu{}_\nu \rangle$ .

Before moving on, consider energy conservation in this model. Suppose there is a symmetry along the timelike vector  $k^\mu$ , i.e.

$$k_{\mu;\nu} + k_{\nu;\mu} = k^\mu \Phi_{;\mu} = 0 \quad (24)$$

It follows that  $\nabla_\mu (k^\nu T^\mu{}_\nu) = 0$ , and the corresponding conserved charge is

$$H = - \int_\Sigma T^\mu{}_\nu k^\nu n_\mu dS, \quad (25)$$

where  $n_\mu$  is the normal to the surface  $\Sigma$ . For the Unruh metric,  $k^t = 1$ ,  $n_t = (ac)^{1/2}$  and  $dS = (a/c)^{1/2} dr$ ,

$$H = - \int_\Sigma a T^t{}_t dr \quad (26)$$

It is possible to verify that this integral is equal to the Hamiltonian of the model, and we read off the physical energy density to be  $-a T^t{}_t$ .

## 5. Fluxes

In this section we solve equations for the stress energy tensor of the Hawking radiation in the long-wavelength limit. In two dimensions, the three components of stress energy, namely the energy density, pressure and flux can be determined from the two conservation laws and the trace anomaly, the latter being the only place where quantum field theory is used [12].

It is convenient to work in the  $(\tau, r)$  coordinate frame where the metric is diagonal. We introduce the energy density  $E(\tau, r)$ , pressure  $P(\tau, r)$  and flux  $F(\tau, r)$ ,

$$E = -\langle T^\tau{}_\tau \rangle, \quad P = \langle T^r{}_r \rangle, \quad F = -\langle T^r{}_\tau \rangle. \quad (27)$$

The energy and momentum conservation law  $\nabla_\mu \langle T^\mu{}_\nu \rangle = (\delta\Gamma/\delta\Phi)\nabla_\nu\Phi$  becomes

$$a\dot{E} = -(aF)' \quad (28)$$

$$aB^{-1}\dot{F} = -(aBP)' + \frac{1}{2}(aB)'(-E+P) + (aB)\Phi' \frac{\delta\Gamma}{\delta\Phi} \quad (29)$$

Note that  $F$  satisfies the usual flux conservation law and  $E$  is the phonon energy density in the laboratory frame if we choose  $a = 1$ . For the present, we remain agnostic on the choice of  $a$ .

The trace anomaly  $T^\mu{}_\mu = -E+P = q(R-6\Phi_{;\mu}\Phi^{;\mu}+4\Phi_{;\mu}{}^\mu)$ , where  $q = \hbar/24\pi$ . For our metric (3),

$$R = \frac{Ba'^2}{a^3} - \frac{Ba''}{a^2} - \frac{a'B'}{a^2} - \frac{B''}{a}, \quad (30)$$

We use the trace anomaly to eliminate the energy density from the equations. Remarkably, the right side of the momentum equation is an exact derivative, and the equations become

$$aB\dot{P} = -B(aF)' \quad (31)$$

$$a\dot{F} = -B(aBP-f)' \quad (32)$$

where

$$f(r) = -\frac{q}{4}B'^2 - \frac{q}{2}\frac{BB'(a\rho)'}{a\rho} - \frac{q}{4}\frac{B^2a'^2}{a^2} - \frac{q}{2}\frac{B^2a'\rho'}{a\rho} + \frac{3q}{16}\frac{B^2\rho'^2 \ln|aB|}{\rho^2} \quad (33)$$

Noting that  $B\partial_r = \partial_{r^*}$ , the equations combine into a wave equation

$$\partial_\tau^2 (aBP-f) - \partial_{r^*}^2 (aBP-f) = 0 \quad (34)$$

Hence the general solution is

$$aBP = \Phi(v) + \Psi(u) + f(r) \quad (35)$$



where  $u = \tau - r^*$  and  $v = \tau + r^*$ . Substituting back for  $F$ ,

$$aF = \Psi(u) - \Phi(v) \quad (36)$$

and for the energy

$$aBE = \Phi(v) + \Psi(u) + h(r) \quad (37)$$

where  $h(r) = f(r) - aB\langle T^\mu{}_\mu \rangle$ ,

$$h(r) = -\frac{q}{4}B'^2 - \frac{q}{2}\frac{BB'(a\rho)'}{a\rho} - \frac{5q}{4}\frac{B^2(a\rho)'^2}{(a\rho)^2} + q\frac{B^2(a\rho)''}{a\rho} + \frac{5q}{8}\frac{B^2\rho'^2}{\rho^2} + qBB'' + \frac{3q}{16}\frac{B^2\rho'^2 \ln|aB|}{\rho^2}. \quad (38)$$

Finally, we want expressions for the energy and fluxes in the physical  $t, r$  coordinate system. Let  $\beta = v_f/c$ , then

$$-T^t{}_t = E - \beta B^{-1}F = -\frac{\beta-1}{aB}\Psi + \frac{\beta+1}{aB}\Phi + \frac{h}{aB} \quad (39)$$

$$T^r{}_r = P - \beta B^{-1}F = -\frac{\beta-1}{aB}\Psi + \frac{\beta+1}{aB}\Phi + \frac{f}{aB} \quad (40)$$

$$-T^r{}_t = F = \frac{1}{a}\Psi - \frac{1}{a}\Phi \quad (41)$$

These are totally general, exact, closed expressions for the quantum stress tensor in the long wavelength limit. However, in practice, we have to integrate (2) and (5) to obtain  $u$  and  $v$  in a given fluid flow, so some numerical computation is necessary.

### 5.1. Boundary conditions for the two-horizon case

So far there are two functions  $\Psi$  and  $\Phi$  which depend on the initial conditions, but also are constrained by regularity conditions at the horizons. In the two-horizon case with linear topology, there are three distinct regions with different coordinate charts for  $u$ . The solution for  $\Psi$  in region  $i$  will be denoted by  $\Psi_i(u)$ . The  $v$  coordinate has the same form in each of the regions, and there is a single function  $\Phi(v)$ .

At the horizons,  $\beta \rightarrow -1$ ,  $B \rightarrow 0$  and  $h \rightarrow -q\kappa^2$ . Regularity of the energy density  $T^t{}_t$  requires that

$$\text{at } r = r_h: \quad \Psi_1(\infty) = \frac{1}{2}q\kappa_h^2 \quad \Psi_2(\infty) = \frac{1}{2}q\kappa_h^2 \quad (42)$$

$$\text{at } r = r_c: \quad \Psi_2(-\infty) = \frac{1}{2}q\kappa_c^2 \quad \Psi_3(-\infty) = \frac{1}{2}q\kappa_c^2 \quad (43)$$

These relations will be sufficient to show that the energy density will increase without limit near the Cauchy horizon whatever the initial conditions. Note that, in the fluid flow, at the horizons  $\kappa_i = c' + v'_f$  and  $v_f = -c$ .

#### 5.1.1. Equal surface gravities

The conditions on  $\Psi_2$  imply that a static solution with  $\Psi_2$  constant can only be achieved when the surface gravities have the same magnitude. In this case, setting  $\Phi = 0$  and  $a = 1$  and  $q = \hbar/24\pi$  gives the Hawking flux  $\kappa^2/48\pi$  for a massless scalar field. It is worthwhile noting here that the flux we obtain implies a flux transmission coefficient  $T = 1$ , when we would expect  $T < 1$ . This odd conclusion is dependent only on the trace anomaly, which is supposed to be independent of the quantum state. It would clearly be desirable to resolve this apparent discrepancy.

We have

$$-T^t_t = -\frac{\beta-1}{48\pi B}\kappa^2 + \frac{h}{B} \quad (44)$$

$$T^r_r = -\frac{\beta-1}{48\pi B}\kappa^2 + \frac{f}{B} \quad (45)$$

$$-T^r_t = \frac{1}{48\pi}\kappa^2 \quad (46)$$

For a circular topology, the constant flux winds around the circle. For the linear topology, we have the unrealistic situation with the flux extending to infinity, due to having a static, and therefore eternal, black hole.

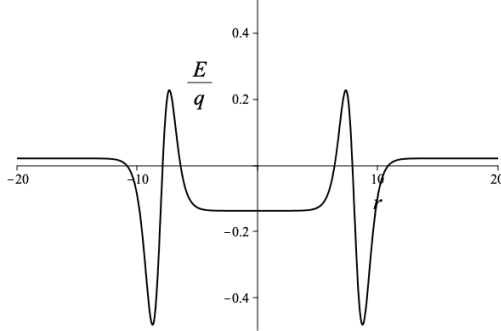


**Figure 5.** Energy density of the Hawking radiation for the two horizon case, with  $|\kappa_c| = |\kappa_h|$ .

A plot of the energy density shows considerable enhancement around each horizon (Figure 5), compared to the asymptotic value. However, the energy is finite, whereas the flow with equal surface gravity can sometimes be unstable to the black hole laser instability [30]. This instability is related to complex roots of the dispersions relation not present in the large wavelength limit we are considering here.

### 5.1.2. Zero flux initial condition

The initial conditions depend in detail on how the experiment is set up. We will consider the case where there is no Hawking flux and no pressure at  $t = 0$ . The initial conditions are then provide restrictions on the  $\Psi$  and  $\Phi$  functions,

$$\Psi_i(u) = -\frac{1}{2}f(r) \text{ at } t = 0 \quad (47)$$

$$\Phi(v) = -\frac{1}{2}f(r) \text{ at } t = 0. \quad (48)$$

In order to use these in the general solution, we have to relate  $u$  and  $v$  to  $r$  and  $t$ . The simplest way of finding explicit expressions for the Hawking flux is to convert  $\Psi$  and  $\Phi$  into partial differential equations. Using  $u = t + r_* - r^*$ , and  $\partial_u \Phi = \partial_v \Psi = 0$ ,

$$\partial_t \Phi = (c - v_f) \partial_r \Phi, \quad (49)$$

$$\partial_t \Psi_i = -(c + v_f) \partial_r \Psi_i. \quad (50)$$

After solving these equations, the functions  $\Psi_i$  and  $\Phi$  are substituted back into the general solutions.

The Hawking flux and the energy density for the flow in Figure 1 are shown in Figure 6 and Figure 7. The flow is moving from the right and the event horizon is also on the right. There are transient bursts of radiation before the flux from the event horizon settles down to the Hawking

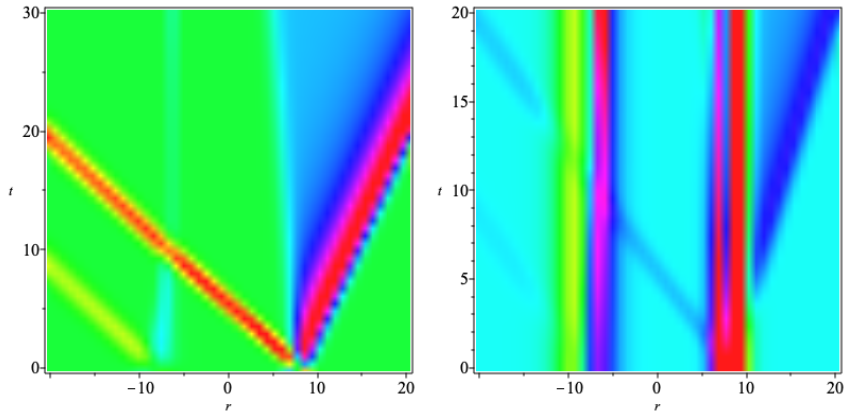


**Figure 6.** Hawking radiation for the two horizon case, with  $|\kappa_c| < |\kappa_h|$  and zero initial flux. The distance unit is the healing length of the sub-luminal region. The Hawking flux is the blue patch emerging from the event horizon (left). The energy density is plotted (right) and shows the concentration around the horizons, although the instability shows up better in the next set of plots.

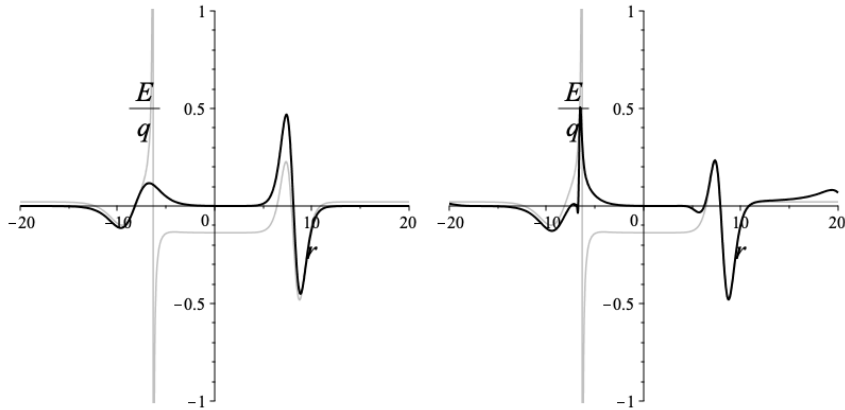


**Figure 7.** The Cauchy horizon instability is shown developing in the energy density from  $t = 0$  (left) to  $t = 20$  (right). The energy density in the sub-luminal regions approaches the static result shown in grey.

value. The energy plots in Figure 7 show the build up of energy at the Cauchy horizon. The grey curve is the static case  $\Phi = 0$ ,  $\Psi = q\kappa_h^2$  which diverges at the Cauchy horizon.

## 6. Conclusion

We have seen how the energy accumulates on the analogue Cauchy horizon in the long wavelength approximation to waves on a BEC. As the energy builds up, the short wavelengths become more important. It then becomes necessary to move on to the complete mode analysis using numerical summation methods. Nevertheless, the scalar dilaton approach gives some analytical insight into the Hawking flux and the relation between an analogue system and Cauchy horizon instability.

## Declaration of interests

The authors do not work for, advise, own shares in, or receive funds from any organization that could benefit from this article, and have declared no affiliations other than their research organizations.

## References

- [1] W. G. Unruh, “Experimental black hole evaporation”, *Phys. Rev. Lett.* **46** (1981), pp. 1351–1353.
- [2] (W. G. Unruh and R. Schützhold, eds.) Eds., *Quantum Analogues: From Phase Transitions to Black Holes and Cosmology*, vol. 718, Lecture Notes in Physics, Springer-Verlag: Berlin Heidelberg, 2007.
- [3] C. Barcelo, S. Liberati and M. Visser, “Analogue gravity”, *Living Rev. Rel.* **8** (2005), article no. 3.
- [4] J. Steinhauer, “Observation of self-amplifying Hawking radiation in an analogue black-hole laser”, *Nat. Phys.* **10** (2014), no. 11, pp. 864–869.
- [5] J. Steinhauer, “Observation of quantum Hawking radiation and its entanglement in an analogue black hole”, *Nature Phys.* **12** (2016), p. 959.
- [6] S. Corley and T. Jacobson, “Black hole lasers”, *Phys. Rev. D* **59** (1999), article no. 124011.
- [7] P. Jain, A. S. Bradley and C. W. Gardiner, “Quantum de Laval nozzle: Stability and quantum dynamics of sonic horizons in a toroidally trapped Bose gas containing a superflow”, *Phys. Rev. A* **76** (2007), no. 2.
- [8] A. Coutant and R. Parentani, “Black hole lasers, a mode analysis”, *Phys. Rev. D* **81** (2009), article no. 084042.
- [9] M. Tettamanti, S. L. Cacciatori, A. Parola and I. Carusotto, “Numerical study of a recent black-hole lasing experiment”, *Eur. Phys. Lett.* **114** (2016), no. 6, article no. 60011.
- [10] J. Steinhauer and J. R. M. de Nova, “Self-amplifying Hawking radiation and its background: a numerical study”, *Phys. Rev. A* **95** (2017), no. 3, article no. 033604.
- [11] Y.-H. Wang, M. Edwards, C. W. Clark and T. Jacobson, “Induced density correlations in a sonic black hole condensate”, *SciPost Phys.* **3** (2017), no. 3, p. 22.
- [12] S. M. Christensen and S. A. Fulling, “Trace Anomalies and the Hawking Effect”, *Phys. Rev. D* **15** (1977), pp. 2088–2104.
- [13] N. D. Birrell and P. C. W. Davies, “On falling through a black hole into another universe”, *Nature* **272** (1978), pp. 35–37.
- [14] P. C. W. Davies and I. G. Moss, “Journey through a black hole”, *Class. Quant. Grav.* **6** (1989), article no. L173.
- [15] E. Poisson and W. Israel, “Internal structure of black holes”, *Phys. Rev. D* **41** (1990), pp. 1796–1809.
- [16] P. R. Brady, I. G. Moss and R. C. Myers, “Cosmic censorship: As strong as ever”, *Phys. Rev. Lett.* **80** (1998), pp. 3432–3435.
- [17] C. Mallery, G. Khanna and L. M. Burko, “Physical objects approaching the Cauchy horizon of a rapidly rotating Kerr black hole”, *Phys. Rev. D* **98** (2018), no. 10, article no. 104024.
- [18] L. M. Burko and A. Ori, “Are physical objects necessarily burnt up by the blue sheet inside a black hole?”, *Phys. Rev. Lett.* **74** (1995), pp. 1064–1066.
- [19] R. Penrose, “Structure of space-time”, in *Battelle rencontres – 1967 lectures in mathematics and physics* (C. M. Dewitt and J. A. Wheeler, eds.), W. A. Benjamin, Inc., 1968.
- [20] L. J. Garay, J. R. Anglin, J. I. Cirac and P. Zoller, “Sonic Analog of Gravitational Black Holes in Bose–Einstein Condensates”, *Phys. Rev. Lett.* **85** (2000), no. 22.
- [21] F. Michel, J.-F. Coupechoux and R. Parentani, “Phonon spectrum and correlations in a transonic flow of an atomic Bose gas”, *Phys. Rev. D* **94** (2016), no. 8, article no. 084027.
- [22] C. G. J. Callan, S. B. Giddings, J. A. Harvey and A. Strominger, “Evanescent black holes”, *Phys. Rev. D* **45** (1992), no. 4, R1005–R1009.
- [23] J. G. Russo, L. Susskind and L. Thorlacius, “Black hole evaporation in (1 + 1)-dimensions”, *Phys. Lett. B* **292** (1992), pp. 13–18.
- [24] R. Balbinot and A. Fabbri, “Hawking radiation by effective two-dimensional theories”, *Phys. Rev. D* **59** (1999), article no. 044031.
- [25] W. Kummer and D. V. Vassilevich, “Hawking radiation from dilaton gravity in (1 + 1)-dimensions: A Pedagogical review”, *Annalen Phys.* **8** (1999), pp. 801–827.
- [26] R. Balbinot, S. Fagnocchi, A. Fabbri and G. P. Procopio, “Backreaction in acoustic black holes”, *Phys. Rev. Lett.* **94** (2004), article no. 161302.
- [27] R. Balbinot, S. Fagnocchi and A. Fabbri, “Quantum effects in acoustic black holes: The Backreaction”, *Phys. Rev. D* **71** (2005), article no. 064019.
- [28] J. S. Dowker, “Conformal anomaly in two-dimensional dilaton scalar theory”, *Class. Quant. Grav.* **15** (1998), pp. 1881–1884.

- [29] R. Bousso and S. W. Hawking, “Trace anomaly of dilaton coupled scalars in two-dimensions”, *Phys. Rev. D* **56** (1997), pp. 7788–7791.
- [30] S. Finazzi and R. Parentani, “Black-hole lasers in Bose-Einstein condensates”, *New J. Phys.* **12** (1998), article no. 095015.